Tailoring silver nanorod arrays for subwavelength imaging of arbitrary coherent sources

Atiqur Rahman,* Pavel A. Belov, and Yang Hao
School of Electronic Engineering and Computer Science, Queen Mary University of London, Mile End Road, London E1 4NS, United Kingdom
(Received 23 July 2010; published 17 September 2010)

The arrays of silver nanorods are known as prospective structures for near-field transmission. However, the available geometries are operating with incoherent sources and do not properly image the coherent ones. In this Brief Report it is demonstrated how the geometry proposed by Ono *et al.* [Phys. Rev. Lett. **95**, 267407 (2005)] can be modified to enable subwavelength imaging of arbitrary coherent sources. The greatly improved performance of the device is demonstrated numerically both through analysis of transmission and reflection coefficients and by full-wave simulation of a particular source imaging.

DOI: 10.1103/PhysRevB.82.113408 PACS number(s): 42.30.−d

The idea to transfer an optical image with subwavelength resolution through a nanolens formed of an array of Ag nanorods was suggested in Ref. 1 and exploits the local excitation of surface plasmon polaritons. An improved multisegment version of this nanolens was suggested in Ref. 2 and promises to offer color imaging and magnification capabilities. In contrast to conventional approach of scanning near-field optical microscopy which involves point-by-point scanning with a single probe, Ono *et al.*[1] and Kawata *et al.*[2] suggested to develop devices capable of operating with distributions of near field with certain aperture, analogous to Pendry's pioneering proposal.[3] Experimental proof of Pendry's proposal is demonstrated in Refs. 4 and 5. A layered metal-dielectric structure[6,7] is also a well-known candidate for subwavelength imaging operation.

A similar idea of subwavelength image transport by arrays of metallic rods is available in microwave[8] and infrared[9,10] domains. As discussed in Ref. 11 by the authors, the proper imaging by such a structure requires the length of rod L to obey Fabry-Pérot (FP) resonance condition $L=n\lambda_g/2$, where λ_g is the guided wavelength and n is an integer number. Similar condition applies to holey metal films as discussed in Ref. 12. However, no such rule that governs the imaging in the visible regime was stated in Refs. 1 and 2. Moreover, the parameters of rods used in Ref. 1 produce anomalous results—the field distribution produced by an incoherent source is transported perfectly, however, the nanolens fails to reproduce the distribution of an arbitrary coherent sources—and therefore, demand further attention that would explain the operation of such a device. This Brief Report unravels the operation principles of the nanolens, thereby paving the way for engineering its performance for arbitrary coherent sources.

Following to the authors experience[11] with such subwavelength imaging devices, it is necessary to know the guided wavelength of the system, in order to have an idea of its regime of operation. The guided wavelength λ_g of a single infinite rod with radius r embedded in a medium having permittivity ϵ_h can be calculated using the following equation:[13]

$$\frac{\gamma_h I_1(\gamma_m r) K_0(\gamma_h r)}{\gamma_m I_0(\gamma_m r) K_1(\gamma_h r)} = -\frac{\epsilon_h}{\epsilon_m}, \tag{1}$$

where $\gamma_{h,m}=\sqrt{\beta^2-\epsilon_{h,m}\mu_0\omega^2}$, ϵ_m is the permittivity of the metal, I_ν and K_ν are the modified Bessel functions.

The above Eq. (1) gives us $\lambda_g=139.43$ nm for a Ag rod of diameter 20 nm in free space at 488 nm wavelength which was used in Ref. 1. The real imaging system however, comprises of a number of finite-size rods arranged in certain lattice configuration and will have a different λ_g than the one calculated for a single infinite-length rod. Therefore, λ_g calculated applying the Eq. (1) gives us only an initial guess about the region where the optima length of rod will lie. Thus, the first FP resonance necessary for proper image formation is expected for the length of rod $L\approx\lambda_g/2=70$ nm, in contrary to 50 nm length originally used in Ref. 1. In order to verify the prediction we have investigated the transmission characteristics for arrays with various lengths of the nanorods (starting from 50 nm with 10 nm increment) and compared their performances. A field of an arbitrary coherent source at the front interface of the array can be expanded into spatial harmonics with transverse wave vectors $\mathbf{k}_t=(0,k_y,k_z)^T$. By ensuring that the transmission coefficient for all these spatial harmonics is close to unity by amplitude and has constant phase, we can guarantee that the system will transmit images of arbitrary coherent sources without distortions.

Figure 1(b) shows the geometry of the nanorod array with triangular lattice pattern which was numerically modeled using commercial full-wave electromagnetic simulator CST™ MICROWAVE STUDIO. We have used the Drude model for permittivity of Ag defined as $\varepsilon_m(\omega)=\varepsilon_\infty-\omega_p^2/(\omega^2+i\Gamma\omega)$ with $\varepsilon_\infty=4.9638$, $\omega_p=1.4497\times10^{16}$ rad/s and $\Gamma=8.33689\times10^{13}$/s (Ref. 1) which gives us the permittivity value of $-9.121+i0.304$ at wavelength of 488 nm.

The transmission coefficient through the infinite array for TM polarization has been calculated employing unit cell shown in Fig. 1(a) with periodic boundary conditions in both y and z directions. Figure 2 shows the transmission coefficient as a function of k_z for various lengths of the nanorods. The calculations have been done for rods with 20 nm diam-

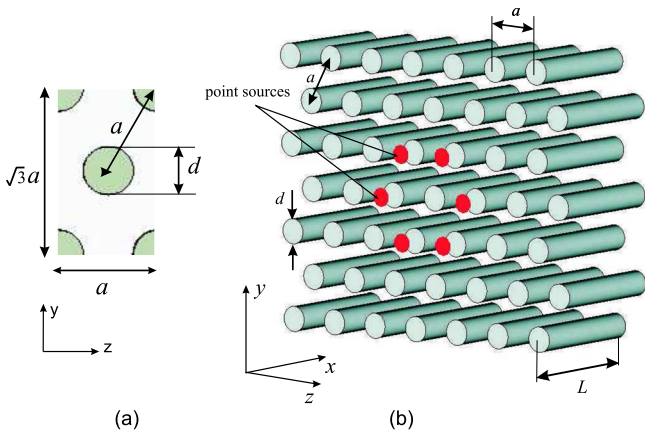

FIG. 1. (Color online) (a) Unit-cell employed to calculate the transmission and reflection coefficients of an infinite array having triangular lattice. (b) Geometry of the finite array of nanorods with triangular-lattice arrangement. The point sources are aligned with the axis of the nanorod and are placed at a distance 10 nm away from array interface. The rod has a length L. E field is sampled across a plane 10 nm away from back interface.

eter, 40 nm period of array, and assuming $k_y=0$ for simplicity. It is interesting to note that while the transmission coefficient of evanescent waves ($k_z > k_0$) significantly varies for various lengths of the rod, the propagating waves ($0 \leq k_z < k_0$) enjoy almost 100% transmission for all considered cases. Thus, in order to retrieve only the propagating waves any of these lengths can be employed. However, in order to reconstruct the image with subwavelength resolution we have to ensure that evanescent harmonics are also recovered. This can be guaranteed by having a resonance-free transmission coefficient characteristics achievable through proper selection of rod length as evinced by Fig. 2.

We started with length $L=50$ nm which was proposed in Ref. 1, and increased it to 100 nm with 10 nm intervals. The transmission pattern for rods with length $L=50$ nm [see Fig. 2(a)] shows resonant amplification for some spatial harmonics. The transmission coefficient for evanescent waves turns out to be greater than unity, but this effect does not violate energy conservation law since evanescent waves does not transport energy in the direction of their decay. Such behavior is well known in microwave[14] and IR (Refs. 10 and 15) ranges and has been identified as the ostensible element that impairs the image. It is necessary to eliminate this resonance feature from the transmission pattern in order to have any discernible image. Figure 2 shows that the resonance gets subdued as the rod length is gradually increased from 50 nm. With the rod length of 80 and 90 nm the resonance amplification almost disappears and transmission pattern gets flatter which is a desirable quality to achieve good subwavelength imaging performance for arbitrary coherent sources. Note that the transmission coefficient curve for $L=90$ nm shows, at higher spatial harmonics ($k_z > 4k_0$), an upward trend which transforms to a resonance (at $k_z \simeq 5.5k_0$) for a rod length of 100 nm. It is understandable that this frail resonance will be stronger for lengths beyond 100 nm. Following to transmission coefficient amplitude analysis, 80- and 90-nm-long rods are optimal candidates for assembly of nanolens capable of operating with arbitrary sources with subwavelength resolution.

The final criterion for the selection of rod length is the transmission phase which is required to be constant over the evanescent harmonic region. Figure 3 shows the transmission and reflection phases obtained for various lengths of the rod. It is evident that a rod length of 80 nm produces least phase variation compared to the others which is a desirable property that guarantees all the evanescent harmonics reach

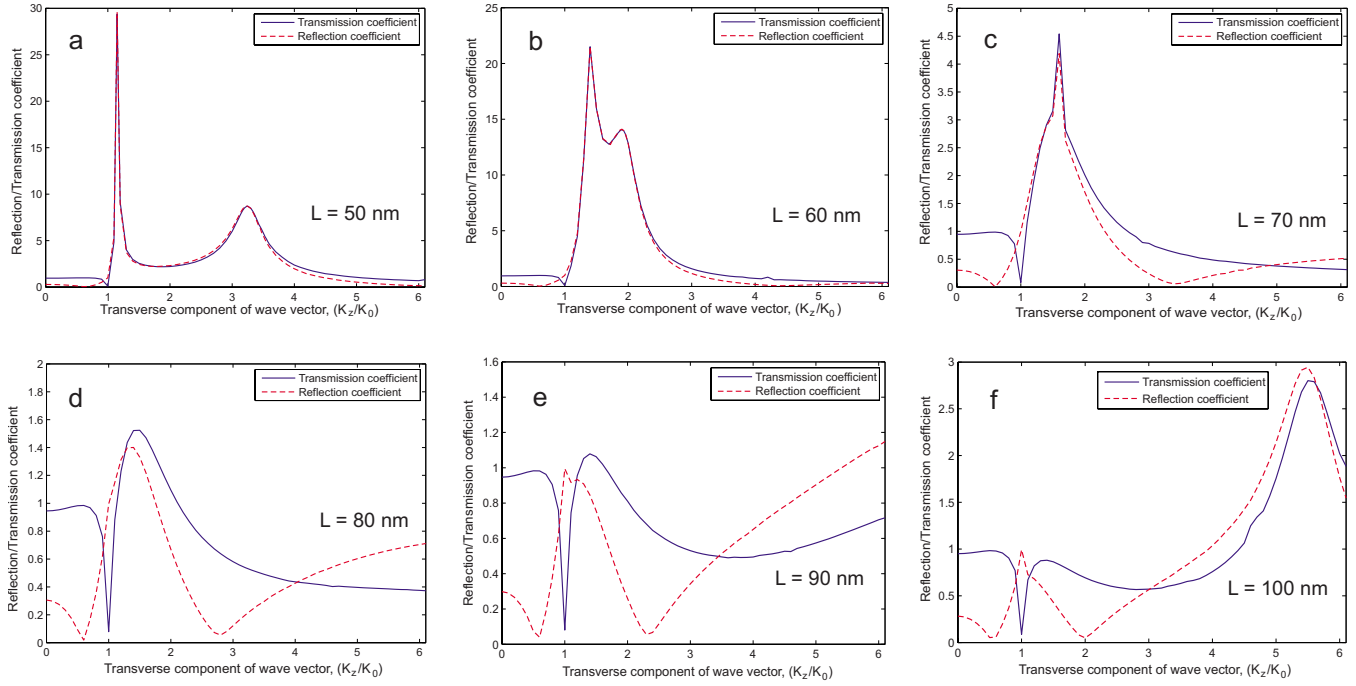

FIG. 2. (Color online) Evolution of transmission coefficient pattern with different lengths of the Ag rod at an operation wavelength of 488 nm. Rod diameter, $d=20$ nm, and periodicity, $a=40$ nm, are kept constant for all these cases.

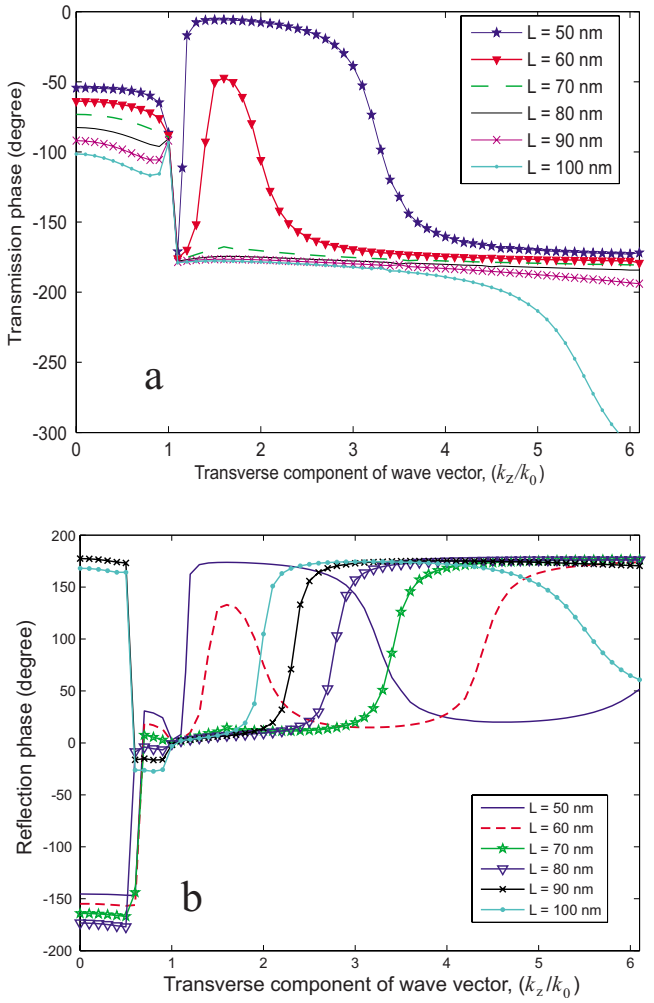

FIG. 3. (Color online) Phase of transmission and reflection coefficients for various lengths of the nanorod.

the other side of the lens simultaneously. Note that in contrast to the phase of transmission coefficient, the reflection coefficient phase exhibits a sudden jump in the evanescent wave region.

Based on the studies of transmission coefficient, we opt for the rod of 80 nm length which, in our opinion, would be the best fit for the purpose of subwavelength imaging of arbitrary coherent sources. The chosen length of rod lies in the vicinity of our original prediction of $L=70$ nm made on the basis of guided wavelength calculation. The difference is attributed to the finite size of the rods (edge effect) and the interactions among them. In order to demonstrate that an array of 80-nm-long rods provides much better imaging performance as compared to geometry in Ref. 1 with a rod length of 50 nm, we tested the imaging capability of this device with discrete coherent source which had the worst image following to Ref. 1. The discrete source formed by six in-phase point sources placed at discrete points forming a hexagon is shown in Fig. 1(b). Each point source is a small dipole polarized along the rod axis (X axis) and placed 10 nm away from the array interface (front interface). The images of this discrete source sampled at the other side of the array (10 nm from the back interface) with various lengths of the

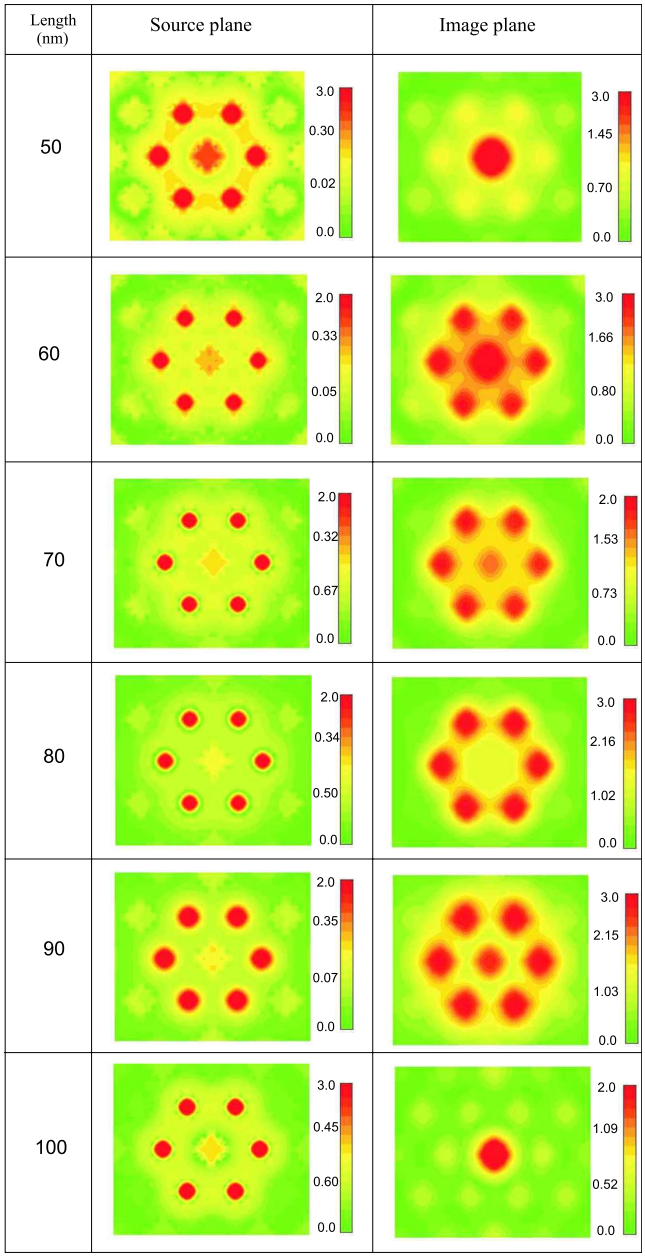

FIG. 4. (Color online) Source and image plane field distribution for various lengths of the rod.

rod are plotted in Fig. 4. The image obtained with 50 nm rod replicates the result of Ref. 1 and does not represent the original source field distribution at all. The image that closely mimics the source is the one obtained with 80 nm rod which supports our earlier decision made on the basis of transmission coefficient calculation. The field distributions at the image plane obtained with 60, 70, and 90 nm rod give us a misleading vision of source comprised of seven dipoles for a bright point, besides the six that represent the source, at the center is discerned. However, 50 and 100 nm rod give us an impression of a source formed of a single dipole located at the center of the hexagon.

In conclusion, we have demonstrated how we can tailor the length of Ag rods in an array in order to ensure subwavelength imaging of arbitrary coherent sources. We have gone

through the rigorous procedure of transmission coefficient calculation followed by the simulation of a finite array excited with particular source in order to justify our decision. It is learnt that a resonance-free transmission coefficient magnitude and constant phase are mandatory to reproduce the source field distribution. Such tailoring can also be done by altering the nanoenvironment of the individual rod, i.e., by having different lattice arrangements and spacings.

The authors would like to thank Andrea Alu of the University of Texas, Austin for useful discussion and acknowledge financial support by EPSRC.

*atiqur.rahman@elec.qmul.ac.uk

[1] A. Ono, J. I. Kato, and S. Kawata, Phys. Rev. Lett. **95**, 267407 (2005).
[2] S. Kawata, A. Ono, and P. Verma, Nat. Photonics **2**, 438 (2008).
[3] J. B. Pendry, Phys. Rev. Lett. **85**, 3966 (2000).
[4] D. S. Melville and R. J. Blaikie, Opt. Express **13**, 2127 (2005).
[5] N. Fang, H. Lee, C. Sun, and X. Zhang, Science **308**, 534 (2005).
[6] S. A. Ramakrishna, J. B. Pendry, M. C. K. Wiltshire, and W. J. Stewart, J. Mod. Opt. **50**, 1419 (2003).
[7] Z. Liu, H. Lee, Y. Xiong, C. Sun, and X. Zhang, Science **315**, 1686 (2007).
[8] P. A. Belov, Y. Zhao, S. Tse, P. Ikonen, M. G. Silveirinha, C. R. Simovski, S. Tretyakov, Y. Hao, and C. G. Parini, Phys. Rev. B **77**, 193108 (2008).
[9] G. Shvets, S. Trendafilov, J. B. Pendry, and A. Sarychev, Phys. Rev. Lett. **99**, 053903 (2007).
[10] M. Silveirinha, P. A. Belov, and C. R. Simovski, Phys. Rev. B **75**, 035108 (2007).
[11] A. Rahman, P. A. Belov, M. G. Silveirinha, C. R. Simovski, Y. Hao, and C. G. Parini, Appl. Phys. Lett. **94**, 031104 (2009).
[12] J. Jung, F. J. Garcia-Vidal, L. Martin-Moreno, and J. B. Pendry, Phys. Rev. B **79**, 153407 (2009).
[13] J. Takahara, S. Yamagishi, H. Taki, A. Morimoto, and T. Kobayashi, Opt. Lett. **22**, 475 (1997).
[14] P. A. Belov and M. G. Silveirinha, Phys. Rev. E **73**, 056607 (2006).
[15] A. Rahman, P. Belov, Y. Hao, and C. G. Parini, Opt. Lett. **35**, 142 (2010).